

# Building a shp: A New Rare-Earth Metal–Organic Framework and its Application in a Catalytic Photo-oxidation Reaction

Victor Quezada-Novoa,<sup>a</sup> Hatem M. Titi,<sup>b</sup> Amy A. Sarjeant, Ashlee J. Howarth<sup>\*a</sup>

<sup>a.</sup> Department of Chemistry and Biochemistry, Concordia University, 7141 Sherbrooke St. W., H4B 1R6, Montreal, Quebec, Canada.

<sup>b.</sup> Department of Chemistry, McGill University, 801 Sherbrooke St. W., H3A 0B8, Montreal, Quebec, Canada.

**Abstract:** The design and synthesis of new metal–organic frameworks (MOFs) is important from both a fundamental and application standpoint. In this work, a novel, highly-connected rare-earth (RE) MOF with **shp** topology is reported, named RE-CU-10 (RE = rare-earth, CU = Concordia University), comprised of nonanuclear RE(III)-cluster nodes and tetratopic pyrene-based linkers. This represents the first time that the 1,3,6,8-tetrakis(*p*-benzoic acid)pyrene (H<sub>4</sub>TBAPy) linker is integrated in the **shp** topology. Y-CU-10 was explored as a heterogeneous photocatalyst for the selective oxidation and detoxification of a sulfur mustard simulant, 2-chloroethyl ethyl sulfide (2-CEES), showing a half-life for conversion to the less toxic 2-chloroethyl ethyl sulfoxide (2-CEESO) of 6.0 min.

## Introduction

Metal–organic frameworks (MOFs) are hybrid materials comprised of metal ions or clusters interconnected by organic linkers, giving rise to open structures with accessible pores.<sup>1–4</sup> MOFs have been studied for many potential applications including, but not limited to, gas adsorption,<sup>5,6</sup> catalysis,<sup>7,8</sup> photocatalysis,<sup>9,10</sup> chemical sensing,<sup>11,12</sup> and wastewater remediation.<sup>13–16</sup> Rare-earth (RE) metals, which include scandium, yttrium and the fifteen lanthanides, have been used to synthesize a diverse library of MOFs, including many with unique structures and properties driven by the high coordination numbers and geometries of RE-metals.<sup>17–20</sup> Like other classes of MOFs, RE-MOFs have been reported with several different secondary building units (SBUs), including inorganic nodes that are metal ions,<sup>21,22</sup> chains,<sup>23–25</sup> or clusters.<sup>5,26–29</sup> In 2013, Eddaoudi *et al.* showed that the use of fluorinated modulators, such as 2-fluorobenzoic acid, favors the formation of RE-cluster nodes, instead of the ion or chain nodes that tend to preferentially form in the presence of carboxylic acid linkers.<sup>18</sup> This includes RE-cluster nodes with high nuclearity and connectivity, giving rise to MOFs with complex and intricate topologies, some of which are likely to be inaccessible with other metals.<sup>29–32</sup> In one example, a MOF with **shp** topology, named RE-**shp**-MOF-1 (RE = Y(III), and Tb(III)) was reported,<sup>33</sup> representing one of two edge transitive (4,12)-c nets where a double six-membered ring (d6R) building block acts as a 12-connected (12-c) node.<sup>34</sup> RE-**shp**-MOF-1 is comprised of square, tetratopic porphyrin-based linkers (5,10,15,20-tetrakis(4-carboxyphenyl)porphyrin, H<sub>4</sub>TCPP) and 12-connected nonanuclear Y(III)-cluster nodes, giving a structure with 1D triangular channels. In another example, RE-**shp**-MOF-5 was reported, comprised of 12-c nonanuclear RE(III)-cluster nodes and rectangular 1,2,4,5-tetrakis(4-

carboxyphenyl)benzene (BTEB) linkers. The same 12-connected nonanuclear RE(III)-cluster was used as a building block in the synthesis of RE-**pek**-MOF-1 (RE = Y(III), and Tb(III)), and RE-**aea**-MOF-1 (RE = Y(III)), when combined with tritopic linkers.<sup>35</sup>

In this work, we report the synthesis of a new RE-MOF, RE-CU-10 (RE = Y(III), Tb(III), CU = Concordia University), with **shp** topology, comprised of nonanuclear RE(III)-cluster nodes and rectangular tetratopic pyrene-based linkers, 1,3,6,8-tetrakis(*p*-benzoic acid)pyrene (H<sub>4</sub>TBAPy) (Figure 1). The **shp** topology has not yet been reported for a MOF comprised of tetratopic H<sub>4</sub>TBAPy linkers, since the use of this linker tends to favor the formation of **scu**, and **csq** topologies driving the formation of 8-connected hexanuclear cluster nodes (NU-901 (**scu**, Zr<sub>6</sub>-cluster),<sup>36,37</sup> Ce-CAU-24 (**scu**, Ce<sub>6</sub>-cluster)<sup>38</sup>, or NU-1000 (**csq**, Zr<sub>6</sub>-cluster or Ce<sub>6</sub>-cluster)).<sup>38,39</sup> Finally, RE-CU-10, with a high density of pyrene chromophores, ~13 Å channels, and high porosity is applied for the photocatalytic oxidation and detoxification of a sulfur mustard simulant, 2-chloroethyl ethyl sulfide (2-CEES).

## Results and Discussion

The combination of the tetratopic linker H<sub>4</sub>TBAPy with Y(III), or Tb(III) in the presence of 2-fluorobenzoic acid (2-FBA) under solvothermal conditions in DMF, yields the MOF, RE-CU-10. Single-crystal X-ray diffraction (SCXRD), shows that RE-CU-10 crystallizes in the trigonal space group *P* $\bar{3}$ m1, comprised of a nonanuclear cluster, which appears as a RE<sub>18</sub> cluster due to disorder (Figure S1 and S2). A similar phenomenon was observed in the metal cluster of PCN-223, a

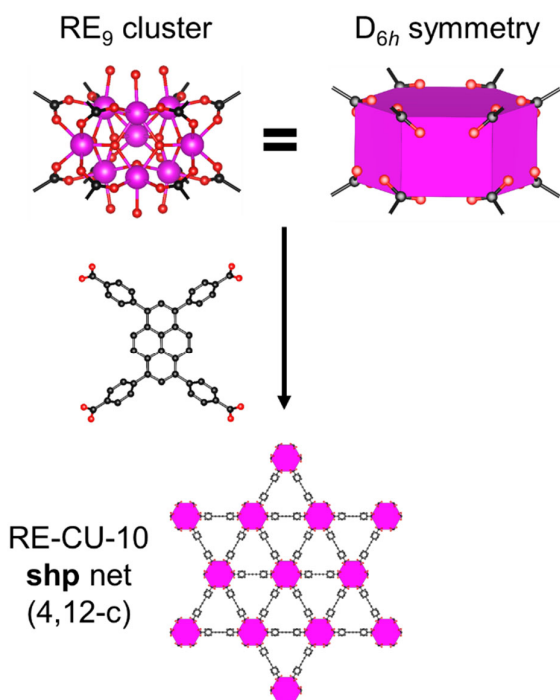


Figure 1. Structure of RE-CU-10, showing the RE<sub>9</sub>-cluster node and 1,3,6,8-tetrakis(*p*-benzoic acid)pyrene linker.

Zr<sub>6</sub>-based MOF comprised of H<sub>4</sub>TCPP linkers with **shp** topology, where the hexanuclear Zr(IV)-cluster was disordered over three positions, appearing as a Zr<sub>18</sub>-cluster.<sup>40</sup> In a different interpretation by Farha *et al.*, the disordered Zr<sub>18</sub>-cluster in NU-904 (**scu** topology) was found to be caused by merohedral twinning in the structure where three **scu** nets overlap, giving six-fold symmetry and the appearance of an **shp** net.<sup>41</sup> It should be noted that the scanning electron microscopy (SEM) images taken of NU-904 show prolate spheroid-shaped particles, indicative of the **scu** topology and different from the hexagonal-shaped particles expected to be observed for MOFs with **shp** topology.<sup>42</sup> Based on SEM images (Figure 2), <sup>1</sup>H-NMR spectroscopy (Figure S3 and S4) and thermogravimetric analysis (TGA) (Figure S5) of RE-CU-10, we conclude that the experimental chemical formula for Y-CU-10 is DMA<sub>3</sub>[Y<sub>9</sub>(μ<sub>3</sub>-OH)<sub>12</sub>(μ<sub>3</sub>-O)<sub>2</sub>(TBAPy)<sub>3</sub>(2-FBA)<sub>2</sub>].2DMF and for Tb-CU-10 is DMA<sub>3</sub>[Tb<sub>9</sub>(μ<sub>3</sub>-OH)<sub>12</sub>(μ<sub>3</sub>-O)<sub>2</sub>(TBAPy)<sub>3</sub>(2-FBA)<sub>2</sub>].(DMF)(2-FBA), confirming the presence of a nonanuclear RE(III)-cluster node, and **shp** topology. Although not all of the bridging hydroxy and/or oxo ligands could be assigned by SCXRD due to the level of disorder in the structure, the cluster possesses similar connectivity and spatial arrangement of RE-metals as the nonanuclear cluster reported in Y-**shp**-MOF-1<sup>33</sup> and pek-MOF-1.<sup>35</sup> Each individual nonanuclear RE(III)-cluster is coordinated by twelve crystallographically independent TBAPy linkers, giving a 12-connected (12-c) node. All carboxylates coordinated to the cluster bridge adjacent RE atoms and arrange to form a d6R hexagonal prism (Figure 1). Structural and topological analysis of the resulting structure shows the formation of a (4,12)-c MOF, building a net with **shp** topology (Figure 1, Figures S6-S10). The carboxylphenyl groups in RE-CU-10 are rotated from

the plane of the pyrene core, showing a dihedral angle of ~58°. This angle is similar or inferior in magnitude compared to other **shp** MOFs made with different tetratopic linkers and nonanuclear RE(III)-clusters (~59° Y-**shp**-MOF-5,<sup>43</sup> ~68° for RE-**shp**-MOF-1),<sup>33</sup> and also similar to the dihedral angle of ~60° found for the same linker in NU-1000 (**csq** topology).<sup>44</sup> This highlights the diversity of topologies that can be made with RE(III)-cluster nodes, owing, in part, to the existence and stability of high nuclearity clusters with somewhat flexible coordination geometries. The structure features one-dimensional triangular channels along the “c” axis of 13 Å in diameter, and 12 Å hexagonal-prismatic cages enclosed by six linkers and two metal clusters (Figure S7 and S8.).

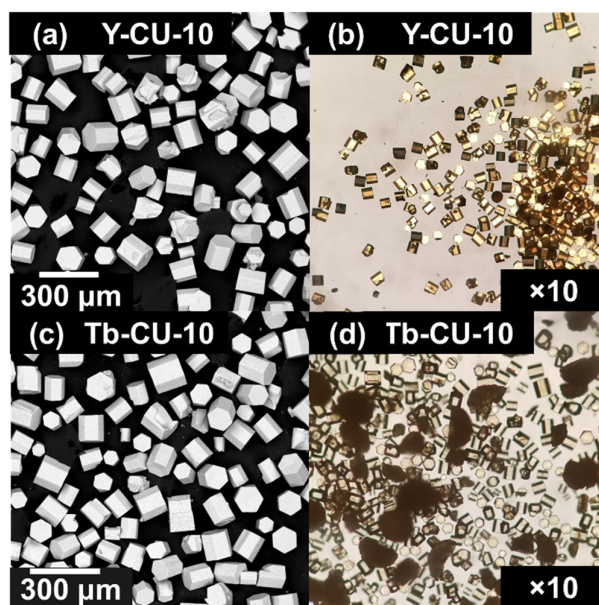


Figure 2. Scanning electron microscopy (SEM) (a, c) and optical microscopy (b, d) images of bulk microcrystalline samples of Y-CU-10 (a, b) and Tb-CU-10 (c, d).

Bulk microcrystalline samples of RE-CU-10 (Figure 2) were synthesized and the phase purity of the product was confirmed by powder X-ray diffraction (PXRD) (Figure 3a). N<sub>2</sub> adsorption analysis showed a reversible type-1 isotherm with a calculated BET surface area (pore diameter) of 1750 m<sup>2</sup>g<sup>-1</sup> (11 Å), and 1780 m<sup>2</sup>g<sup>-1</sup> (11 Å) for Y-, and Tb-CU-10, respectively (Figure 3b, Figure S11), after activation under vacuum at 120 °C. Scanning electron microscopy shows the characteristic hexagonal-prismatic microcrystals derived from the trigonal space group, and as expected for a MOF with **shp** topology. Diffuse reflectance infrared Fourier transform spectroscopy (DRIFTS) shows the expected absorption bands from the symmetric and asymmetric carboxylate stretching (Figure S12), as well as O-H stretching bands corresponding to μ<sub>3</sub>-OH ligands in the nonanuclear RE(III)-cluster node. Thermogravimetric analysis (TGA) of activated samples of RE-CU-10 under air (Figure S5) shows that RE-CU-10 is stable up to 450 °C, comparable to other RE-cluster-based MOFs.<sup>33,43</sup> <sup>1</sup>H-NMR spectroscopy of digested

samples of RE-CU-10 shows the presence of the TBAPy linker, DMF and 2-FBA modulator (Figure S3 and S4).

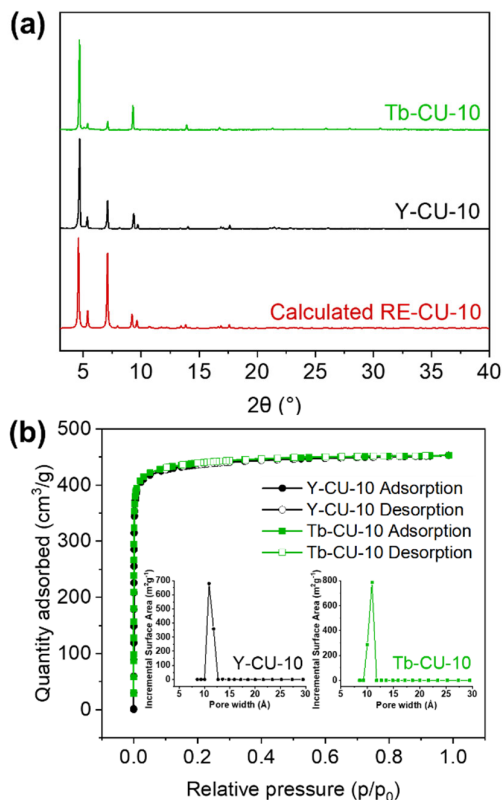


Figure 3. (a) Simulated and experimental PXRD patterns of RE-CU-10, and (b) nitrogen adsorption-desorption isotherms of RE-CU-10 (inset: pore size distribution plots)

Given that RE-CU-10 has a moderate density of pyrene chromophores (3 pyrene linkers per RE<sub>9</sub>-node) coupled with 13 Å channels that can aid in diffusion of reactants and products, we expected the MOF to perform well in the selective oxidation of the sulfur mustard simulant 2-CEES to 2-CEESO. Sulfur mustard is a chemical warfare agent that was used for the first time during WWI. Unfortunately it is still a potential threat for public health today, due to its stockpiling and potential production from nations that have not signed or followed ratification of the Chemical Weapons Convention treaty (CWC).<sup>45</sup> Sulfur mustard is a very reactive alkylating agent which causes the failure of cellular functions,<sup>46</sup> presenting as a strong blistering agent that causes acute and chronic injuries to the skin, eyes and respiratory system.<sup>47,48</sup> Sulfur mustard accumulated in facilities or present in inadequate disposal sites must be destroyed in an efficient and controlled manner, and one method to safely detoxify the compound involves selective oxidation to its nontoxic sulfoxide derivative.

In 2015, Hupp, Farha *et al.* demonstrated that the sulfur mustard simulant, 2-CEES could be selectively oxidized and detoxified to the less toxic 2-CEESO, by using the MOF PCN-

222/MOF-545 as a photosensitizer to generate singlet oxidation under LED irradiation.<sup>49</sup> The group has since studied several different pyrene-containing MOFs for the degradation of 2-CEES and sulfur mustard, including NU-1000 (**csq**)<sup>50,51</sup>, postsynthetically modified NU-1000 (**csq**)<sup>52,53</sup> and NU-400 (**fcu**).<sup>54</sup> These materials are comprised of hexanuclear Zr(IV)-cluster nodes, and tetratopic or ditopic pyrene-based linkers in NU-1000 and NU-400, respectively. In all cases, the linker behaves as a photosensitizer for the generation of singlet oxygen, under LED irradiation, which subsequently selectively oxidizes 2-CEES.

Activated samples of Y-CU-10 were suspended in methanol in a microwave vial and purged with oxygen for 30 minutes. 2-CEES and the internal standard, mesitylene, were added and the mixture was excited using a UV LED photoreactor ( $\lambda_{max} = 390-400$ , see details in SI). Under optimized conditions, using 0.9 mol% of Y-CU-10 as a catalyst (1.728  $\mu\text{mol}$ ), CEES can be completely selectively oxidized to CEESO within 15 min (half-life 6.0 min) (Figure 4b). GC-FID analysis indicates that no sulfone product was formed during the process. The half-life for the selective oxidation of 2-CEES by Y-CU-10 is comparable to that reported for NU-1000 (6.2 min half-life), a MOF with fewer pyrene chromophores per node (2 pyrene linkers per Zr<sub>6</sub>-node) but larger 30 Å channels. This result demonstrates the trade-off between higher pyrene chromophore density vs. pore aperture size.

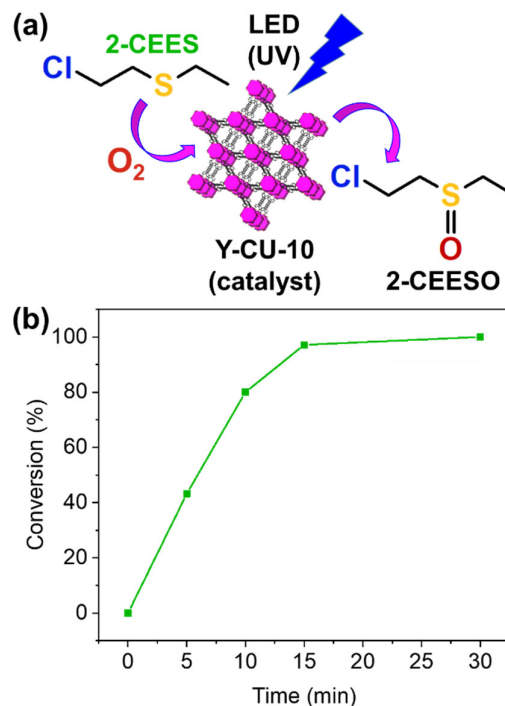


Figure 4. (a) Conversion of 2-CEES to 2-CEESO using Y-CU-10 as a catalyst under UV-LED irradiation, (b) conversion vs. time for the selective oxidation of 2-CEES, as determined by GC-FID analysis.

## Conclusions

The ability of rare-earth metals to form high nuclearity clusters, coupled with their versatile coordination numbers and geometries allows for the synthesis of structures that are not as easily accessible with d-block metals. In this report, the nonanuclear RE(III)-cluster which acts as a d6R node, enables the synthesis of RE-CU-10, a MOF with **shp** topology comprised of TBAPy linkers – a linker that has not yet been observed in the **shp** topology. RE-CU-10 demonstrates permanent porosity, with surface areas of 1750–1780 m<sup>2</sup>/g, and thermal stability in air up to 450 °C. In addition, the moderate density of pyrene chromophores per mole along with the microporosity of Y-CU-10, allows for the moderately fast, and selective photocatalytic oxidation and detoxification of a sulfur mustard simulant, 2-CEES, at low catalytic loadings (0.9 mol%), with a conversion half-life of only 6 min.

## Conflicts of interest

There are no conflicts to declare.

## Acknowledgements

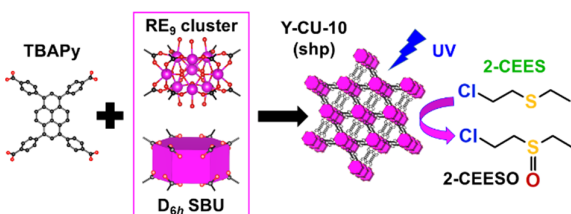
V.Q. thanks Concordia University for the Anne Harper Pallen Entrance Scholarship, the Concordia International Tuition Award of Excellence, the Howarth and Majewski research group members for offering a friendly and supportive research environment. V.Q. also thanks Prof. Majewski for helpful discussion regarding organic synthetic techniques. V.Q. and A.J.H. thank Prof. Tomislav Friščić for access to PXRD and scXRD facilities, Petr Fiurasek (Centre québécois sur les matériaux fonctionnels) for help with TGA, Prof. Yves Gélinas for access to and help with GC-FID measurements, and Dr. David Polcari (Systems for Research) for access to the Phenom benchtop SEM instrument. We acknowledge the support of the Natural Sciences and Engineering Research Council of Canada (NSERC), [funding reference number: DGECR-2018-00344]. Cette recherche a été financée par le Conseil de recherches en sciences naturelles et en génie du Canada (CRSNG), [numéro de référence: DGECR-2018-00344].

## Notes and references

- 1 B. F. Hoskins and R. Robson, *J. Am. Chem. Soc.*, 1989, **111**, 5962–5964.
- 2 G. Férey, C. Mellot-Draznieks, C. Serre, F. Millange, J. Dutour, S. Surblé and I. Margiolaki, *Science*, 2005, **309**, 2040–2042.
- 3 M. Kondo, T. Yoshitomi, H. Matsuzaka, S. Kitagawa and K. Seki, *Angew. Chem. Int. Ed.*, 1997, **36**, 1725–1727.
- 4 H. Furukawa, K. E. Cordova, M. O’Keeffe and O. M. Yaghi, *Science*, **341**, 1230444.
- 5 H. He, D. Yuan, H. Ma, D. Sun, G. Zhang and H.-C. Zhou, *Inorg. Chem.*, 2010, **49**, 7605–7607.
- 6 S. Roy, A. Chakraborty and T. K. Maji, *Coord. Chem. Rev.*, 2014, **273–274**, 139–164.
- 7 J. Lee, O. K. Farha, J. Roberts, K. A. Scheidt, S. T. Nguyen and J. T. Hupp, *Chem. Soc. Rev.*, 2009, **38**, 1450–1459.

- 8 M. Rimoldi, A. J. Howarth, M. R. DeStefano, L. Lin, S. Goswami, P. Li, J. T. Hupp and O. K. Farha, *ACS Catal.*, 2017, **7**, 997–1014.
- 9 Q. Wang, Q. Gao, A. M. Al-Enizi, A. Nafady and S. Ma, *Inorg. Chem. Front.*, 2020, **7**, 300–339.
- 10 J.-L. Wang, C. Wang and W. Lin, *ACS Catal.*, 2012, **2**, 2630–2640.
- 11 C. A. Bauer, T. V. Timofeeva, T. B. Settersten, B. D. Patterson, V. H. Liu, B. A. Simmons and M. D. Allendorf, *J. Am. Chem. Soc.*, 2007, **129**, 7136–7144.
- 12 L. E. Kreno, K. Leong, O. K. Farha, M. Allendorf, R. P. Van Duyne and J. T. Hupp, *Chem. Rev.*, 2012, **112**, 1105–1125.
- 13 P. A. Kobielska, A. J. Howarth, O. K. Farha and S. Nayak, *Coord. Chem. Rev.*, 2018, **358**, 92–107.
- 14 A. J. Howarth, Y. Liu, J. T. Hupp and O. K. Farha, *Cryst. Eng. Comm.*, 2015, **17**, 7245–7253.
- 15 S. Rojas and P. Horcajada, *Chem. Rev.*, 2020 ASAP article.
- 16 R. J. Drout, L. Robison, Z. Chen, T. Islamoglu and O. K. Farha, *Trends. Chem.*, 2019, **1**, 304–317.
- 17 S. Fordham, X. Wang, M. Bosch and H.-C. Zhou, *Lanthanide Metal-Organic Frameworks*, Springer Berlin Heidelberg, Berlin, Heidelberg, Peng Cheng., 2014, vol. 163.
- 18 D.-X. Xue, A. J. Cairns, Y. Belmabkhout, L. Wojtas, Y. Liu, M. H. Alkordi and M. Eddaoudi, *J. Am. Chem. Soc.*, 2013, **135**, 7660–7667.
- 19 J. Luo, H. Xu, Y. Liu, Y. Zhao, L. L. Daemen, C. Brown, T. V. Timofeeva, S. Ma and H.-C. Zhou, *J. Am. Chem. Soc.*, 2008, **130**, 9626–9627.
- 20 F. Saraci, V. Quezada-Novoa, R. P. Donnarumma and A. J. Howarth, *Chem. Soc. Rev.*, "in review"
- 21 S.-Y. Zhang, W. Shi, P. Cheng and M. J. Zaworotko, *J. Am. Chem. Soc.*, 2015, **137**, 12203–12206.
- 22 H. S. Quah, L. T. Ng, B. Donnadieu, G. K. Tan and J. J. Vittal, *Inorg. Chem.*, 2016, **55**, 10851–10854.
- 23 M. Kumar, L.-H. Wu, M. Kariem, A. Franconetti, H. N. Sheikh, S.-J. Liu, S. C. Sahoo and A. Frontera, *Inorg. Chem.*, 2019, **58**, 7760–7774.
- 24 T. Devic, C. Serre, N. Audebrand, J. Marrot and G. Férey, *J. Am. Chem. Soc.*, 2005, **127**, 12788–12789.
- 25 Y. Cui, H. Xu, Y. Yue, Z. Guo, J. Yu, Z. Chen, J. Gao, Y. Yang, G. Qian and B. Chen, *J. Am. Chem. Soc.*, 2012, **134**, 3979–3982.
- 26 Z. Chen, P. Li, X. Zhang, P. Li, M. C. Wasson, T. Islamoglu, J. F. Stoddart and O. K. Farha, *J. Am. Chem. Soc.*, 2019, **141**, 2900–2905.
- 27 G. K. Angeli, C. Sartsidou, S. Vlachaki, I. Spanopoulos, C. Tsangarakis, A. Kourtellaris, E. Klontzas, G. E. Froudakis, A. Tasiopoulos and P. N. Trikalitis, *ACS Appl. Mater. Interfaces*, 2017, **9**, 44560–44566.
- 28 F. Gándara, E. Gutiérrez-Puebla, M. Iglesias, N. Sneško and M. Á. Monge, *Cryst. Growth. Des.*, 2010, **10**, 128–134.
- 29 H. Jiang, J. Jia, A. Shkurenko, Z. Chen, K. Adil, Y. Belmabkhout, L. J. Weselinski, A. H. Assen, D.-X. Xue, M. O’Keeffe and M. Eddaoudi, *J. Am. Chem. Soc.*, 2018, **140**, 8858–8867.
- 30 A. H. Assen, Y. Belmabkhout, K. Adil, P. M. Bhatt, D.-X. Xue, H. Jiang and M. Eddaoudi, *Angew. Chem. Int. Ed.*, 2015, **54**, 14353–14358.
- 31 O. Yassine, O. Shekhah, A. H. Assen, Y. Belmabkhout, K. N. Salama and M. Eddaoudi, *Angew. Chem. Int. Ed.*, 2016, **55**, 15879–15883.
- 32 R. Luebke, Y. Belmabkhout, Ł. J. Weseliński, A. J. Cairns, M. Alkordi, G. Norton, Ł. Wojtas, K. Adil and M. Eddaoudi, *Chem. Sci.*, 2015, **6**, 4095–4102.
- 33 Z. Chen, Ł. J. Weseliński, K. Adil, Y. Belmabkhout, A. Shkurenko, H. Jiang, P. M. Bhatt, V. Guillerme, E. Dauzon, D.-X. Xue, M. O’Keeffe and M. Eddaoudi, *J. Am. Chem. Soc.*, 2017, **139**, 3265–3274.
- 34 O. Delgado-Friedrichs, M. O’Keeffe and O. M. Yaghi, *Acta Crystallogr. A.*, 2006, **62**, 350–355.

- 35 D. Alezi, A. M. P. Peedikakkal, Ł. J. Weseliński, V. Guillerm, Y. Belmabkhout, A. J. Cairns, Z. Chen, Ł. Wojtas and M. Eddaoudi, *J. Am. Chem. Soc.*, 2015, **137**, 5421–5430.
- 36 C.-W. Kung, T. C. Wang, J. E. Mondloch, D. Fairen-Jimenez, D. M. Gardner, W. Bury, J. M. Klingsporn, J. C. Barnes, R. Van Duyne, J. F. Stoddart, M. R. Wasielewski, O. K. Farha and J. T. Hupp, *Chem. Mater.*, 2013, **25**, 5012–5017.
- 37 S. J. Garibay, I. Iordanov, T. Islamoglu, J. B. DeCoste and O. K. Farha, *Cryst. Eng. Comm.*, 2018, **20**, 7066–7070.
- 38 S. Smolders, A. Struyf, H. Reinsch, B. Bueken, T. Rhauderwiek, L. Mintrop, P. Kurz, N. Stock and D. E. D. Vos, *Chem. Commun.*, 2018, **54**, 876–879.
- 39 J. E. Mondloch, W. Bury, D. Fairen-Jimenez, S. Kwon, E. J. DeMarco, M. H. Weston, A. A. Sarjeant, S. T. Nguyen, P. C. Stair, R. Q. Snurr, O. K. Farha and J. T. Hupp, *J. Am. Chem. Soc.*, 2013, **135**, 10294–10297.
- 40 D. Feng, Z.-Y. Gu, Y.-P. Chen, J. Park, Z. Wei, Y. Sun, M. Bosch, S. Yuan and H.-C. Zhou, *J. Am. Chem. Soc.*, 2014, **136**, 17714–17717.
- 41 J. Lyu, X. Zhang, K. Otake, X. Wang, P. Li, Z. Li, Z. Chen, Y. Zhang, M. C. Wasson, Y. Yang, P. Bai, X. Guo, T. Islamoglu and O. K. Farha, *Chem. Sci.*, 2019, **10**, 1186–1192.
- 42 J. Jiao, D. Jiang, F. Chen, D. Bai and Y. He, *Dalton Trans.*, 2017, **46**, 7813–7820.
- 43 R. G. AbdulHalim, P. M. Bhatt, Y. Belmabkhout, A. Shkurenko, K. Adil, L. J. Barbour and M. Eddaoudi, *J. Am. Chem. Soc.*, 2017, **139**, 10715–10722.
- 44 P. Li, Q. Chen, T. C. Wang, N. A. Vermeulen, B. L. Mehdi, A. Dohnalkova, N. D. Browning, D. Shen, R. Anderson, D. A. Gómez-Gualdrón, F. M. Cetin, J. Jagiello, A. M. Asiri, J. F. Stoddart and O. K. Farha, *Chem*, 2018, **4**, 1022–1034.
- 45 United Nations Treaty Collection, [https://treaties.un.org/Pages/ViewDetails.aspx?src=TREATY&mtdsg\\_no=XXVI-3&chapter=26&lang=en](https://treaties.un.org/Pages/ViewDetails.aspx?src=TREATY&mtdsg_no=XXVI-3&chapter=26&lang=en), (accessed 27 March 2020).
- 46 K. Kehe, F. Balszuweit, D. Steinritz and H. Thiermann, *Toxicology*, 2009, **263**, 12–19.
- 47 M. Rowell, K. Kehe, F. Balszuweit and H. Thiermann, *Toxicology*, 2009, **263**, 9–11.
- 48 K. Ghabili, P. S. Agutter, M. Ghanei, K. Ansarin, Y. Panahi and M. M. Shoja, *Crit. Rev. in Toxicol.*, 2011, **41**, 384–403.
- 49 Y. Liu, A. J. Howarth, J. T. Hupp and O. K. Farha, *Angew. Chem. Int. Ed.*, 2015, **54**, 9001–9005.
- 50 Y. Liu, C. T. Buru, A. J. Howarth, J. J. Mahle, J. H. Buchanan, J. B. DeCoste, J. T. Hupp and O. K. Farha, *J. Mater. Chem. A*, 2016, **4**, 13809–13813.
- 51 C. T. Buru, M. B. Majewski, A. J. Howarth, R. H. Lavroff, C.-W. Kung, A. W. Peters, S. Goswami and O. K. Farha, *ACS Appl. Mater. Interfaces*, 2018, **10**, 23802–23806.
- 52 A. J. Howarth, C. T. Buru, Y. Liu, A. M. Ploskonka, K. J. Hartlieb, M. McEntee, J. J. Mahle, J. H. Buchanan, E. M. Durke, S. S. Al-Juaid, J. F. Stoddart, J. B. DeCoste, J. T. Hupp and O. K. Farha, *Chem. Eur. J.*, 2017, **23**, 214–218.
- 53 A. Atilgan, T. Islamoglu, A. J. Howarth, J. T. Hupp and O. K. Farha, *ACS Appl. Mater. Interfaces*, 2017, **9**, 24555–24560.
- 54 G. Ayoub, M. Arhangelskis, X. Zhang, F. Son, T. Islamoglu, T. Friščić and O. K. Farha, *Beilstein J. Nanotechnol.*, 2019, **10**, 2422–2427.



TOC Graphic